Journal of Power Sources 196 (2011) 264–269

Contents lists available at ScienceDirect

Journal of Power Sources

journal homepage: www.elsevier.com/locate/jpowsour

Investigation of the effects of compression pressure on direct methanol fuel cell

Yingli Zhu[a], Chong Liu[a,b,*], Junsheng Liang[a], Liding Wang[a,b]

[a] Key Laboratory for Micro/Nano Technology and System of Liaoning Province, Dalian University of Technology, No. 2, Linggong Road, Dalian, Liaoning Province 116023, China
[b] Key Laboratory for Precision and Non-traditional Machining Technology of Ministry of Education, Dalian University of Technology, Dalian, Liaoning Province 116023, China

ARTICLE INFO

Article history:
Received 7 April 2010
Received in revised form 10 June 2010
Accepted 10 June 2010
Available online 19 June 2010

Keywords:
Direct methanol fuel cell
Compression pressure
Loading history
Feeding mode

ABSTRACT

Compression pressure has significant influence on the performance of direct methanol fuel cell (DMFC) and the effect of compression is more significant for a DMFC than a proton exchange membrane fuel cell (PEMFC). But there are few data concerning the compression pressure on the performance of DMFCs. Loading history and feeding mode may also affect the optimal compression pressure for the DMFC. This paper investigates the influence of compression pressure on the DMFC. The effects of reload and air feeding mode are also examined. The optimal pressure of the DMFC is 1 MPa when the cell is assembled for the first time in forced convection mode. However, the optimum pressure decreases to 0.05 MPa when the cell is compressed again because of the residual strain of the GDL. The optimal pressure decreases to 0.5 MPa when the cell operates in air-breathing mode. Therefore, the optimum compression pressure for a DMFC strongly depends on the loading history and the feeding mode.

1. Introduction

The individual components of a proton exchange membrane fuel cell (PEMFC), namely catalyst-coated membrane (CCM), gas diffusion layers (GDLs) and current collectors (CC) must be held together with sufficient compression pressure to prevent leaking of the reactants and to minimize the contact resistance between those layers [1]. Many experimental and numerical works [2–7] have been carried out to investigate the effects of compression on the electrochemical performance of PEMFCs. Experiments have showed that insufficient compression pressure may result in large contact resistance, and too much pressure may block the fuel transport and even damage the membrane electrode assembly (MEA). In both cases, it will decrease the cell performance. So, there exists an optimum compression pressure for a PEMFC. This optimum pressure depends on the physical properties of the GDL and the gasket. Compared to the PEMFC, the direct methanol fuel cell (DMFC) have advantages of high energy density, reduced size and weight, facile construction, instantaneous refueling and ease of storage of the fuel, which make the DMFC a more promising candidate for portable power systems [8]. However, there are few data concerning the compression pressure on the performance of DMFCs. Furthermore, compression pressure on PEMFCs or DMFCs was controlled by setting the thickness of gasket or measuring the torque of bolts in most literatures [2–5,9]. These control methods for packaging of fuel cell were not precise and were hard to manipulate.

On the other hand, for GDL, the first compression stroke exhibited a different signal than successive strokes because of the weakening of the material during its compression for the first time. Therefore, GDL cannot recover to their initial thickness when the load is removed and exhibits a residual strain [10]. It can be deduced that DMFCs with GDL show different performances when compressed with repeated loading. As far as the author is aware, there is no data concerning this issue. Moreover, mass transport in the GDL of the DMFC is more complex than that of the PEMFC because liquid methanol must be transported through the GDL and carbon dioxide must continuously be removed to avoid blockage of the reaction area [11]. The mass transport strongly depends on the porosity of the GDL and feeding method. Therefore, the effect of compression is more significant for a DMFC than a PEMFC and the operating conditions may also influence the numerical value of the optimal compression pressure applied on DMFC [12]. An effective approach to explore the information of the influence is electrochemical impedance spectroscopy (EIS). Mueller et al. [13,14] indicated that overall impedance of DMFC consists of three parts: the high-frequency arc results from the resistance of the membrane; the medium-frequency arc results from the impedance caused by the resistance of methanol electro-oxidation and oxygen reduction reaction; the low-frequency arc is ascribed to mass transfer of methanol and air.

In this paper we investigate the effects of compression pressure on direct methanol fuel cell. The compression pressure can be controlled precisely and can be applied continuously on the DMFC by an integrated platform. The output performance and the internal resistance of the DMFC were measured by polarization curve and EIS, respectively. The air was separately supplied to the

* Corresponding author. Tel.: +86 411 84707946; fax: +86 411 84707940.
E-mail address: chongl@dlut.edu.cn (C. Liu).

0378-7753/$ – see front matter © 2010 Elsevier B.V. All rights reserved.
doi:10.1016/j.jpowsour.2010.06.034

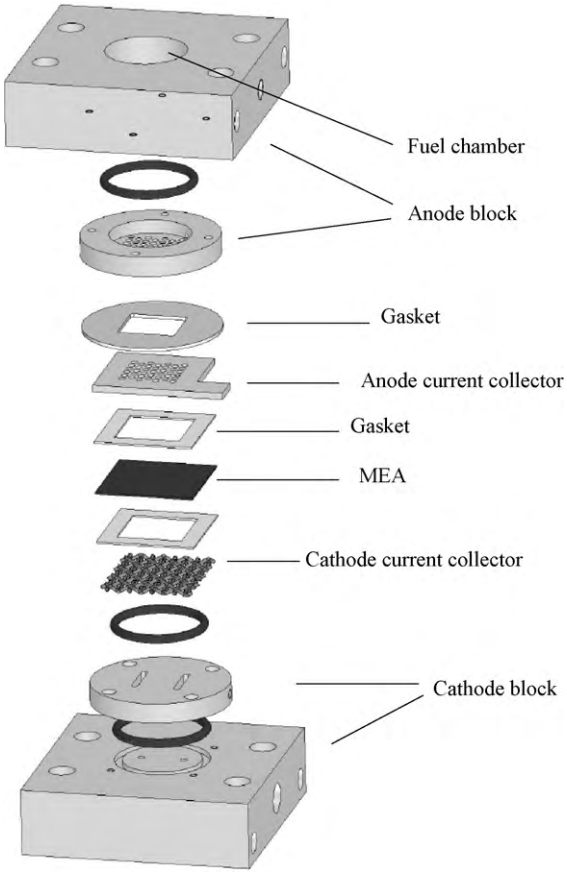

Fig. 1. Schematic of the DMFC and the locations of the components.

cathode of the DMFC by two modes: forced convection and air-breathing. In order to investigate whether the performance of the DMFC depended on loading history, the experiment was carried out again after unloading. Experimental results showed that optimum compression pressure for the DMFC strongly depended on the feeding mode and that the DMFC degraded when it was compressed again.

2. Experimental

2.1. Cell preparation

A piece of catalyst-coated membrane (CCM) with an active surface area of 1.4 cm × 1.4 cm consists of a Nafion 115 membrane, anode catalyst layer of PtRu black (4.5 mg cm^{-2}) and cathode catalyst layer of Pt black (2.4 mg cm^{-2}). The CCM was sandwiched between two telfonised carbon papers (TGP-H-090, Toray), which served as gas diffusion layers (GDLs), and then hot-pressed at 140 °C and 30 atm for 2 min to form the MEA. Gaskets (FJ011, GORE-TEX®) with a thickness of 0.2 mm were used at both anode and cathode of the MEA. The anode current collector used in this experiment was made of stainless steel (SS 316L) sheet with a thickness of 400 μm. An array of circular holes (1 mm diameter) was photochemically etched as fuel feed path. The cathode current collector was a titanium nitride (TiN) plated stainless steel mesh. A fuel chamber, which acted as methanol reservoir, was machined in the anode block that is attached to the DMFC. Gas passage was machined in the cathode block to supply air to the cell. The detailed locations of the components are shown in Fig. 1.

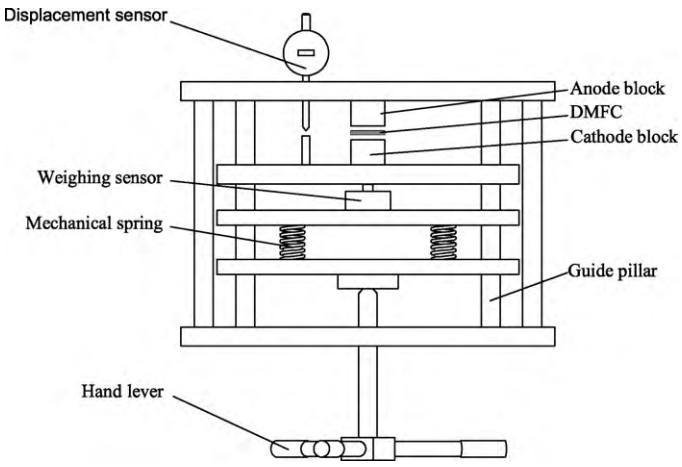

Fig. 2. Schematic presentation of the platform hardware.

2.2. Experimental setup

As depicted in Fig. 2, an integrated platform using rolling pillar and sleeve as guiding device was designed in order to investigate the influence of compression pressure on performance of the DMFC. In this test stand, compression pressure was applied by rotating the hand lever manually. A weighing sensor and a digimatic micrometer were used to measure the applied pressure and displacement, respectively. The precision of displacement and pressure measurement are ±7 μm and ±0.6 kg, respectively. Mechanical springs were used for more accurate pressure and displacement control. The indication error of displacement and pressure control is less than ±2 μm and ±0.2 kg, respectively.

2.3. Measurements

In this experiment, the flow rate of air was 60 ml min^{-1} which was sufficient excessive stoichiometric flow. Incoming air passed in to the cell through a hole in the cathode block and out from another hole. Aqueous methanol with a concentration of 3 M was supplied passively from the fuel chamber in the anode block. The cell was heated by four cylindrical heating elements placed in the holes of the anode and cathode blocks. A thermocouple used to regulate the cell heating is located in the middle of the two heating elements. The cell was thermostatically controlled to 40 °C with an accuracy of ±1 °C during the experiment. The polarization curve and Nyquist plot of the cell were obtained on a DC electronic load and electrochemical station, respectively. The polarization curves were obtained by the constant voltage method. The Nyquist plot was measured at an operating voltage of 0.2 V by EIS at frequencies from 100 kHz to 0.01 Hz. The compression pressure was calculated by dividing the compression force by the current collector area. The performance of the DMFC was tested once when the compression pressure was increased 0.1 MPa. All operating conditions were kept constant during the experiment with the exception of compression pressure except Section 3.4.

3. Results and discussion

3.1. Performance of DMFC at lower compression pressure (below 1 MPa)

Fig. 3 shows the polarization curves of the DMFC on different compression pressures below 1 MPa. With increase of the compression pressure, the output power increased rapidly. As the compression pressure increased from 0 MPa to 1 MPa, the peak

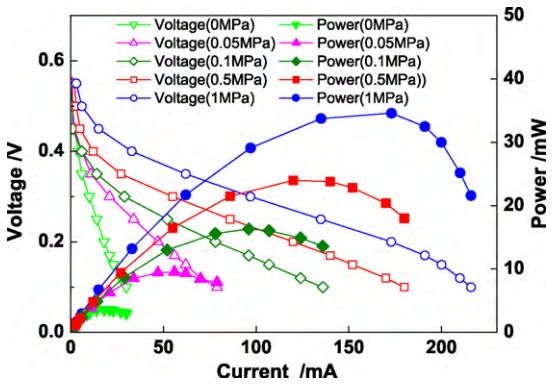

Fig. 3. Performance of the DMFC on different compression pressures (below 1 MPa). At methanol concentration 3 M, air flow rate 60 ml min^{-1}, cell temperature 40 °C.

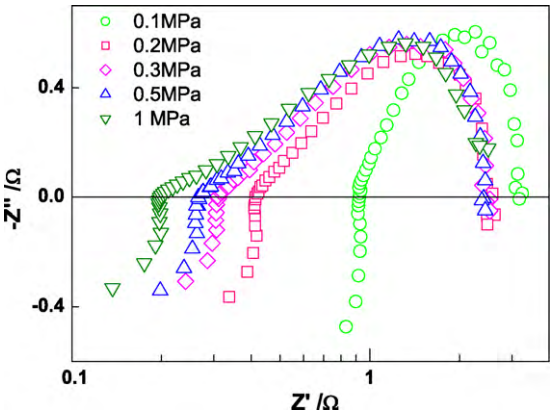

Fig. 4. Nyquist plot of the DMFC on pressure below 1 MPa. At methanol concentration 3 M, air flow rate 60 ml min^{-1}, cell temperature 40 °C, cell voltage 0.2 V.

power increased from 3.5 mW to 32.5 mW. This was because the contact resistance between the layers of the DMFC components decreased with increase of compression pressure (Fig. 4). The total ohmic internal resistance decreased from 8 Ω at 0 MPa to 0.2 Ω at 1 MPa (Fig. 5). The total ohmic resistance of the cell was sum of the bulk resistance of the individual components and contact resistance between the components. When the cell was compressed, the contact resistance declined rapidly while the bulk resistance decreased slightly. The power consumption on the internal resistance of the DMFC decreased and consequently the output power increased. This indicated that the ohmic resistance is a major source of losses at lower compression pressure, which was also been detected by Ihonen et al. [15].

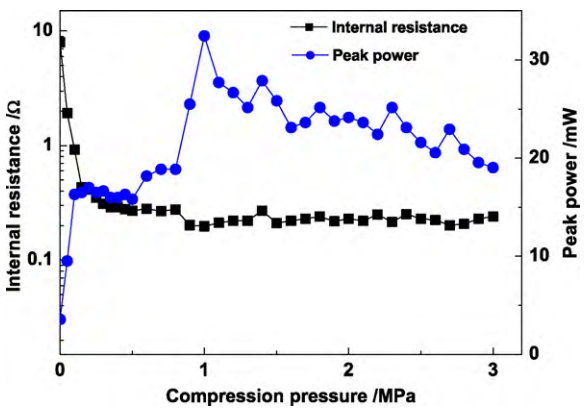

Fig. 5. Internal resistance and peak power with different compression pressures.

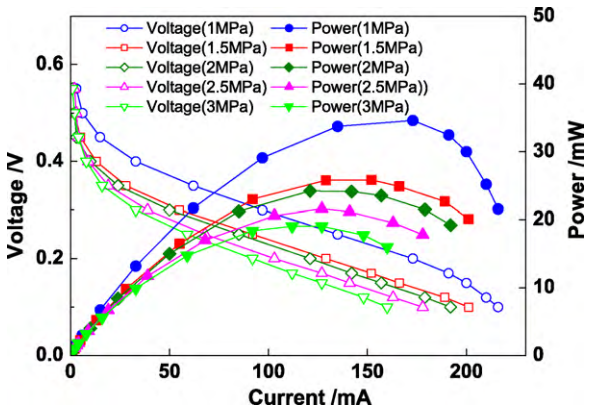

Fig. 6. Performance of the DMFC on different compression pressures (between 1 MPa and 3 MPa). At methanol concentration 3 M, air flow rate 60 ml min^{-1}, cell temperature 40 °C.

3.2. Performance of DMFC at higher compression pressure (above 1 MPa)

When the applied compression pressure exceeded 1 MPa, the output performance of the cell dropped gradually (shown in Fig. 6). However, the internal resistance was almost constant at a level of 0.2 Ω (Fig. 5). Fig. 7 shows Nyquist plot of the cell at pressure above 1 MPa. It can be seen that at the low-frequency (below 1 Hz), the arc became larger with the pressure increase. This indicated that the mass transfer resistance had a remarkably positive correlation with compression pressure. So, the decline of the performance was because the mass transfer resistance in MEA increased as the applied pressure increased. The output performance of the fuel cell depends on the influence of compression pressure in two opposite manners, namely internal ohmic resistance and mass transfer resistance. At lower compression pressure, the ohmic resistance plays a dominant role due to the large contact resistance. But at higher compression pressure, the mass transfer resistance becomes more dominant than internal resistance due to the low porosity of GDL. The optimum compression pressure for this cell was 1 MPa in this experiment. This numerical value was a trade-off between the internal resistance and transfer resistance.

Assuming that the volume of the GDL matrix remains constant, the porosity under compression can be calculated by this equation [16]:

$$\varepsilon = 1 - \frac{d_0}{d}(1 - \varepsilon_0) \quad (1)$$

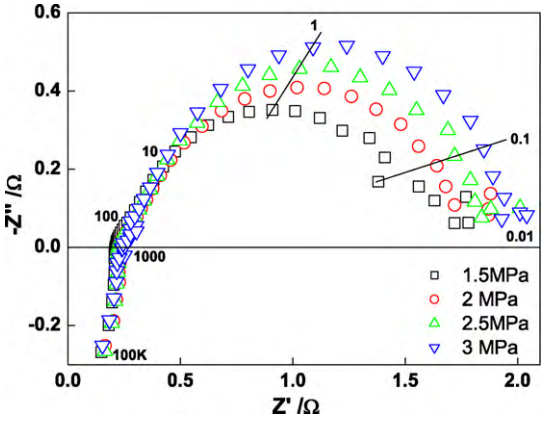

Fig. 7. Nyquist plot of the cell (above 1 MPa). At methanol concentration 3 M, air flow rate 60 ml min^{-1}, cell temperature 40 °C, cell voltage 0.2 V.

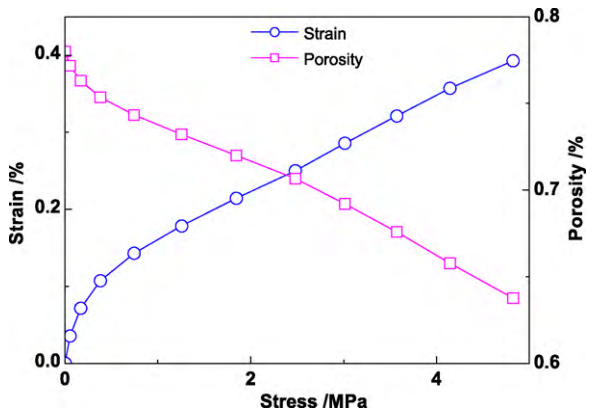

Fig. 8. Relationship between porosity and compression pressure of GDL.

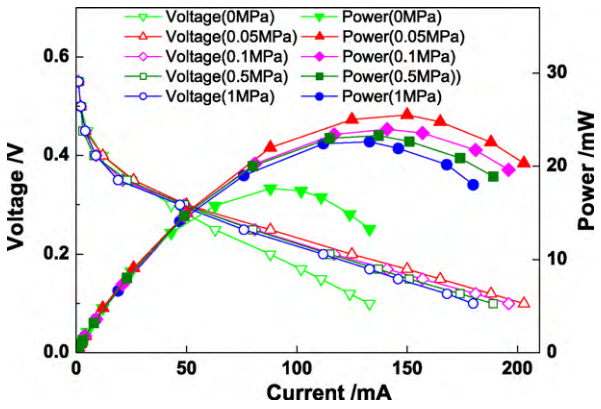

Fig. 10. Performance of the reloaded DMFC. At methanol concentration 3 M, air flow rate 60 ml min^{-1}, cell temperature 40 °C.

where ε is the current porosity, ε_0 is the initial porosity (78%), d is the current thickness, and d_0 is the initial thickness (280 μm). Because the deformation of the sealing gaskets between components of the cell was larger than that of the GDL, it was difficult to measure the current thickness d of the GDL *in situ*. The current thickness d of GDL was obtained from the strain–stress curve (shown in Fig. 8) which was got in another experiment. This experiment was performed to study only the relationship between the strain and compression stress of the GDL. Fig. 8 depicts the effect of compression pressure on the porosity and thickness of the GDL (TGP-H-090). It is shown that the porosity of the GDL is inversely proportional to the compression pressure. As the compression pressure increased to 3 MPa, the porosity decreased to 69% from 78%. It can also be seen that the porosity of GDL was 74% and the thickness was reduced by 15% when pressure was 1 MPa. Considering the inhomogeneous compression of GDL, the local porosity may be even lower.

Fig. 9 is the photograph of the MEA after experiment. It is clear that the patterns of the current collectors were stamped on the GDL and some carbon fibers were fractured at the edge of the holes due to the high compression pressure. Severe inhomogeneous compression can also be observed in the photograph. This illuminated that too high pressure may damage the GDL of MEA and that the holes of current collector must be uniformly distributed to alleviate the inhomogeneous compression.

3.3. Performance of DMFC under reloaded pressure

After the cell was tested as mentioned above, the clamping pressure was completely released and the current collectors and MEA were separated. Then these components were assembled and clamped again. Figs. 10 and 11 are the polarization curve and internal resistance of the reloaded DMFC, respectively. It can be seen that

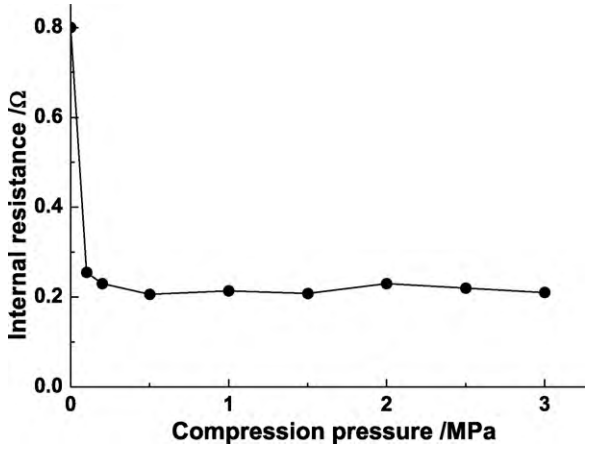

Fig. 11. Internal ohmic resistance of the reloaded DMFC.

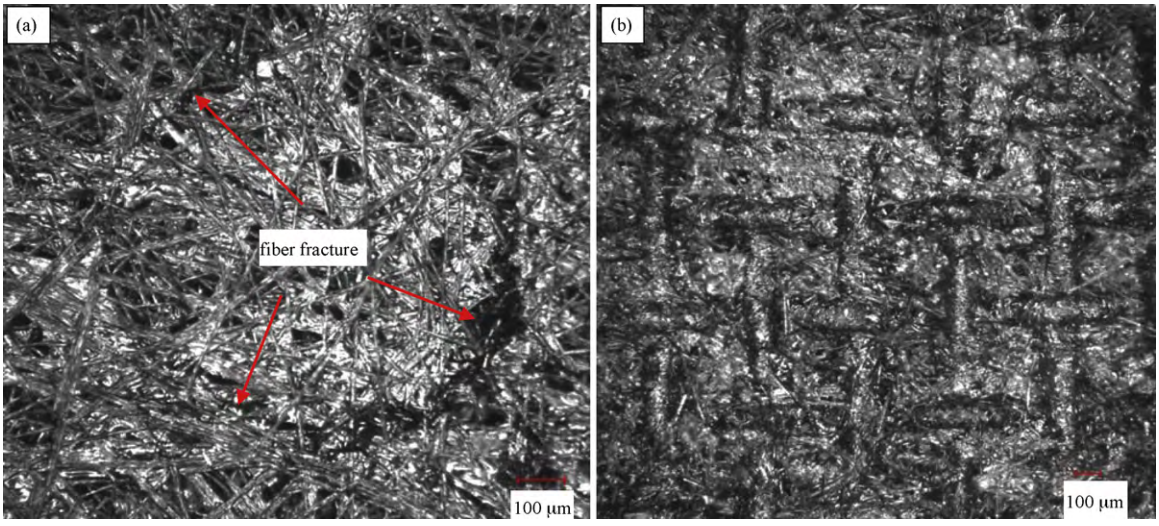

Fig. 9. Photograph of the MEA after experiment: (a) anode side and (b) cathode side.

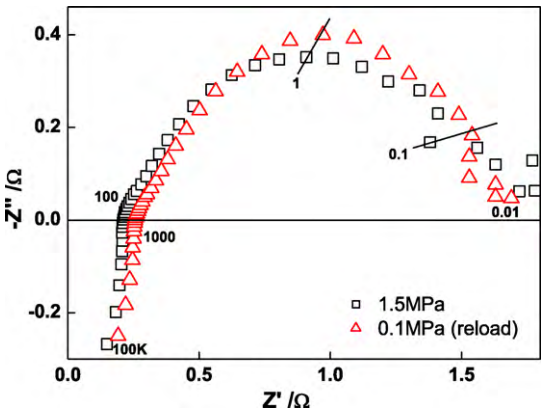

Fig. 12. Nyquist plot comparison of the DMFC between the first and repeated loading.

the internal resistance drop sharply to 0.26 Ω once the compression pressure was 0.05 MPa. At this pressure, the optimum performance (peak power of 25.5 mW) was obtained in the second load cycle. As the pressure increased, the internal resistance further decreased to 0.2 Ω while the output performance decreased gradually. According to Fig. 10, in the low current range (below 50 mA), the output voltage and power on different pressure were almost the same. But in the high current range (above 100 mA), the output performance on different pressures was greatly different because more fuel and oxygen were needed at a high discharge current. Fig. 12 shows the Nyquist plot of the cell at pressure of 0.1 MPa (reload) and 1.5 MPa (former load). It can be seen that the mass transfer resistances (low-frequency arc) was almost the same at the two cases. This indicated that the distortion of the MEA was permanent and the topographical feature of the MEA was unrecoverable. So, the high mass transfer resistance limited the output performance when the cell was compressed again.

3.4. Influence of air feeding mode

In this section, the DMFC was tested in air-breathing mode. The cathode block (shown in Fig. 1) was replaced by a stainless steel sheet which was the same as the anode current collector. The other operation conditions were the same as mentioned above. Figs. 13 and 14 are the polarization curves and Nyquist plot of the DMFC on different compression pressures, respectively. Comparing with Fig. 3, the performance of the air-breathing cell was poor. At 0.1 MPa and 0.2 MPa, the performance of the cell was low because the internal resistance was too high. And the performance was also low at 1 MPa because the mass transfer resistance was too

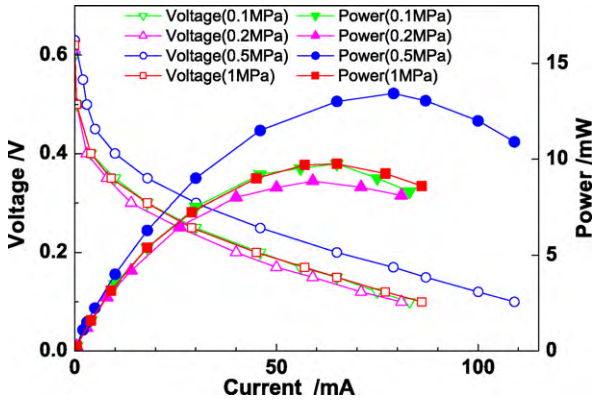

Fig. 13. Performance of the DMFC in air-breathing mode. At methanol concentration 3 M, air-breathing, cell temperature 40 °C.

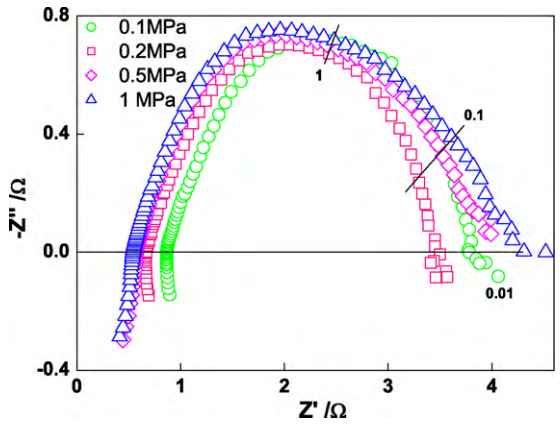

Fig. 14. Nyquist plot of the cell in air-breathing mode. At methanol concentration 3 M, air-breathing, cell temperature 40 °C, cell voltage 0.2 V.

high. As can be seen in Fig. 14, the diameter of the low-frequency arc increased rapidly as the pressure increased. So, 0.5 MPa (the optimal pressure) was also a trade-off between the internal resistance and transfer resistance, which was remarkably lower than that of the cell in forced convection mode. On the other hand, high compression pressure aggravated cell flooding [15], which further increased mass transfer resistance. In forced convection mode, the water generated in the cathode can be eliminated in time, while the flooding in the cathode was more serious in air-breathing mode. It can also be seen from Fig. 8 that the compression percentage of the GDL is 12% when the pressure is 0.5 MPa. So it can be concluded that mild compression was beneficial to air-breathing DMFC. Ge [12] also observed similar phenomenon. In their work, they found that the optimal performance of the DMFC occurred at GDL compression ratio of 12% when the air flow rate was 2000 ml min^{-1} while the optimal performance occurred at 7% when the air flow rate was 1200 ml min^{-1} and 600 ml min^{-1}.

4. Conclusions

In this study the influence of compression pressure on the DMFC was investigated. A testing platform was manufactured to control compression pressure applied on the DMFC precisely. The effects of reload and air feeding mode on the DMFC were examined for the first time. The performance of the cell decreased sharply when it was compressed again because of the permanent distortion of the MEA. The optimal pressure was 1 MPa when the DMFC was tested at an air flow rate of 60 ml min^{-1}, while the optimum pressure was 0.5 MPa in air-breathing mode. It is clear that optimum compression pressure for the DMFC strongly depends on the loading history and feeding mode. So the pressure should be controlled accurately during packaging of a DMFC. More detailed work on this issue should be done in the future.

Acknowledgments

This research is supported by the National Natural Science Foundation of China (No. 50805013, No. 50575036) and Natural Science Foundation of Liaoning Province (No. 20042144). We would also like to thank Prof. Gongquan Sun, Dalian Institute of Chemical Physics of CAS, for providing the required MEA.

References

[1] Frano Barbir, Fuel Cell Stack Design Principles with Some Design Concepts of Micro–Mini Fuel Cells, Mini–Micro Fuel Cells, Springer Science Business Media B.V, 2008.

[2] Woo-kum Lee, Chien-Hsien Ho, J.W. Van Zee, Mahesh Murthy, J. Power Sources 84 (1999) 45–51.
[3] Fang-Bor Weng, Ay Su, Yur-Tsai Lin, et al., ASME J. Fuel Cell Sci. Tech. 2 (2005) 197–201.
[4] W.R. Chang, J.J. Hwang, F.B. Weng, S.H. Chan, J. Power Sources 166 (2007) 149–154.
[5] C. Lim, C.Y. Wang, J. Power Sources 113 (2003) 145–150.
[6] P. Zhou, C.W. Wu, G.J. Ma, J. Power Sources 163 (2007) 874–881.
[7] Z.Y. Su, C.T. Liu, H.P. Chang, et al., J. Power Sources 183 (2008) 182–192.
[8] S.K. Kamarudin, W.R.W. Daud, S.L. Ho, U.A. Hasran, J. Power Sources 163 (2007) 743–754.
[9] C.Y. Chen, J.Y. Shiu, Y.S. Lee, J. Power Sources 159 (2006) 1042–1047.
[10] W. Vielstich, A. Lamm, H.A. Gasteiger, Diffusion media materials and characterisation, in: M. Mathias, J. Roth, J. Fleming, W. Lehnert (Eds.), Handbook of Fuel Cells-Fundamentals, Technology and Applications, vol. 3: Fuel Cell Technology and Applications, John Wiley & Sons Ltd, New Jersey, 2003, Chapter 46.
[11] A. Oedegaard, C. Hebling, A. Schmitz, et al., J. Power Sources 127 (2004) 187–196.
[12] Jiabin Ge, Doctoral Dissertation, University of Miami, 2005.
[13] J.T. Muller, P.M. Urban, J. Power Sources 75 (1998) 139–143.
[14] J.T. Muller, P.M. Urban, W.F. Holderich, J. Power Sources 84 (1999) 157–160.
[15] Jari Ihonen, Mikko Mikkola, Goran Lindbergh, J. Electrochem. Soc. 151 (2004) A1152–A1161.
[16] Matthias Mta, Matthias Rzepkaa, Ulrich Stimminga, J. Power Sources 191 (2009) 456–464.